Scan-to-BIM to Enable Deep Exterior Wall Insulation Retrofits: Promise and Pitfalls

Nathan Catell, Fraunhofer USA Center for Manufacturing Innovation
John C. Briggs, Fraunhofer USA Center for Manufacturing Innovation
Sam Brookfield, Fraunhofer USA Center for Manufacturing Innovation
Aaron Sharpe, Fraunhofer USA Center for Manufacturing Innovation
Kurt Roth, Fraunhofer USA Center for Manufacturing Innovation
Andre Sharon, Fraunhofer USA Center for Manufacturing Innovation

ABSTRACT

Prefabrication of a set of insulated wall panels customized to individual buildings has the potential to dramatically reduce the cost and time to implement exterior wall insulation retrofits. Realizing this vision requires rapidly and accurately identifying the numerous edges of building features and quantifying opaque wall area dimensions. Analysis of point-cloud data from laser scans of buildings has the potential to achieve these goals. Although theoretically straightforward, in practice developing a robust Scan-to-BIM (S2B; BIM = Building Information Model) process that can precisely locate hundreds of edges per building for the highly heterogeneous building stock with minimal human intervention is challenging.

We developed a complete S2B process comprising: 1) Building scanning; 2) Scan registration and point cloud pre-processing; 3) Point cloud segmentation (by object class); and 4) Edge detection, fitting, identification, and 5) Panelization. We discuss these steps and their application to the prefabricated recladding application, including challenges that must be overcome to realize high-quality S2B. To test S2B performance, we compared 48 key dimensions, i.e., wall and window widths and heights, calculated by S2B to conventional measurements for five homes. The S2B matched tape measurements within ±6 mm for all 48 dimensions, with an average absolute difference of 2.5 mm, demonstrating effective S2B is possible.

Introduction

Numerous prior studies have identified exterior wall insulation retrofits as a key measure for reducing residential space conditioning energy consumption in colder climates. For example, PNNL (2022) estimated that applying ~R-24 insulation to the exterior walls of a DOE prototypical single-family home in different climates would reduce whole-home space conditioning energy consumption by 34% to 38% and 16 to 21% for homes lacking wall insulation and homes with dense-pack cellulose already in the wall cavity, respectively. When applied to pre-2000 1- to 4-family U.S. homes in mixed, cold, and very cold climates, this measure has national annual site energy savings potential of ~750 TBtu (Briggs et al. 2022).

Currently, market-viable approaches to add inches of exterior insulation to walls do not exist for the 1- to 4-family homes that account for a large majority of housing units and residential HVAC energy consumption. The state-of-the art process requires extensive high-skill labor to achieve acceptable finishes at the interface of the insulation and the control layers at wall penetrations and connections (windows, doors, pipes, porches, vents, electrical boxes, etc.), making it prohibitively expensive and disruptive (BSC 2013, PNNL 2022).

Technology development efforts have focused on offsite prefabrication of a complete set of retrofit panels customized to the unique geometry of each building (e.g., PNNL 2022, Briggs et al. 2022, Highland Park Technologies 2026). This requires accurate characterization of the opaque wall area to be clad, i.e., its dimensions and different edge types (which determines the design of each panel's edge to interface with the trim installed at terminations). Once this task is complete, a panelization tool can solve for the set of panels to clad each facade, given constraints on panel sizes, minimum and maximum panel sizes, manufacturing cost functions, etc.

To realize this vision, organizations have worked to develop processes to automate acquisition of building dimensions with high fidelity. Although some have worked on photogrammetric approaches (e.g., Gilmour and Stroulia 2022, Borkowski and Kubrat 2024), most have focused on using laser LiDAR (light detection and ranging) scans of building facades to generate a wire frame building information model (BIM) of facades, i.e., scan-to-BIM (see, for example, Xiong et al. 2013; Esfahani et al. 2021; Briggs et al. 2022; Egan, Fouquet, and Harris 2023; Maldonado Puente, Hayes, and Hun 2023; Rauch and Brauml 2023; Selvakumar et al. 2025; Signetron 2026). In theory, one could attempt manual scan-to-BIM, picking individual points from the point cloud generated by the scans to precisely trace out every edge. In practice, this is very difficult, as one must select points among the millions and millions of points, which is often not intuitive in the rendering of the three-dimensional point cloud on a two-dimensional screen. Numerous outlier and "phantom" points, as well as the sheer number of edges that must be found for all but the simplest facades, further complicates manual processing. As a result, a high-quality manual scan-to-BIM process that fully characterizes all facades of a building is very time and labor intensive, requiring high skill and patience, making it not scalable.

Our paper provides an overview of an automated scan-to-BIM approach focused on the application of recladding the walls of smaller buildings with smaller prefabricated insulated panels (e.g., 1' high by 4' long, Briggs et al. 2022). We first discuss the steps of the scan-to-BIM process, describing important challenges encountered and ways to mitigate them. We then show the performance of the complete scan-to-BIM process applied to five buildings.

The Scan-to-BIM Process

The Scan-to-BIM (S2B) process comprises several steps:

1. Building Scanning;
2. Scan Registration and Point Cloud Pre-processing;
3. Point Cloud Segmentation;
4. Edge Detection, Fitting, Identification; and
5. Panelization.

Figure 1 shows the progression from a fully registered point cloud (left) to identification and fitting of wall edges for different terminations (middle; most are windows, wall corners, and soffits) and panelization (right). The panelization process also generates unique CAD files for each panel incorporating the features required for each edge that enables offsite panel prefabrication.

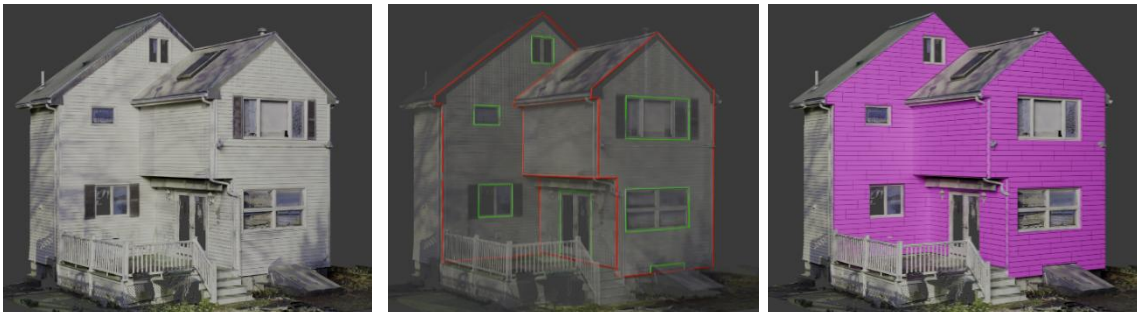

Figure 1. The Scan-to-BIM progression from a registered point cloud of a building (left) to a surface wireframe of the opaque wall area with all edges identified (middle) to fully panelized walls (right).

The subsequent subsections discuss the steps of the S2B process in further detail, highlighting important challenges can arise.

Building Scanning

A terrestrial laser scanner is mounted on a tripod and a building scan is performed. The scanner (Leica RTC360 for the authors) uses a time-of-flight laser sensor to measure the distance from the scanner to a point on the building. A fast-rotating mirror and slower rotating stage allows nearly complete 360x360° spherical distance measurement. Following the laser scan, three cameras take images at eight different angles and the images are used to estimate the appropriate RGB color for each point found in the point cloud. The result is a single colorized point cloud showing all the building features viewable from that location, aka *setup*.

To get a more complete point cloud of the building, the operator moves the scanner and tripod to additional locations (setups) and perform additional scans. The technician chooses the scan locations so that all key building features (e.g., walls) are visible to the scanner. These individual point clouds, as shown in the left three images of Figure 2, document only a section of the building. Properly aligning, or registering, scans from the individual setups to each other is a critical step. Different targets can be used in the field, such as spheres or barcodes, to help in the post-processing of the setups. The Leica uses a second set of cameras, called VIS (Visual Inertial System), to track the relative scan locations and keep them roughly registered to each other.

Figure 2. Lidar scans taken from several different locations and the unified point cloud from all locations.

Scan Registration and Point Cloud Pre-Processing

Postprocessing software (e.g., Register360 for Leica) accurately aligns each scan (setup) to the other scans, using algorithms that minimize error between overlapping point clouds. In brief, the software aligns the point clouds from individual setups by identifying common elements in both scans and then finding the alignment that minimizes the difference in location of those features between the scans. Terrestrial LiDAR scanners often capture points over a full 360^o of rotation, so objects not targeted in scans can support (e.g., a solid, fixed sidewalk) or degrade (e.g., wind-blown tree branches that move between setups) registration. In addition, transient objects that appear in one scan (or a portion of one scan) but not another, such as cars and people, can affect registration quality. Scan accuracy also decreases with distance, so the software may eliminate more distant points when another, closer scan captures the same points. An additional issue in scans is reflected images, i.e., laser scanning near a reflective object, such as window glass, can cause “ghost” images in the point clouds. Manual post-processing editing can eliminate these errors, while wise choices of scanning locations can minimize their importance, e.g., avoid scanning next to a sliding glass patio door.

There are several parameters that can be varied in the registration process and several metrics for evaluating registration quality. Two important ones are: 1) Overlap: The percentage of overlapping points between scans (higher is better); and 2) Bundle Error: The absolute average mean misalignment between scans across all the scans registered together (i.e., the bundle). Lower is better, with the target varying with the application and data requirements.

Once registered to each other (far right in Figure 2), the point cloud is exported as a single, unified point cloud for the S2B process. The postprocessing software implements other important functions such as eliminating some suspect points and trimming out unneeded parts of the point cloud such as neighboring houses.

Figure 3 below shows how poor scan registration can compromise point cloud quality. The subpar scan (left) complicated registration, resulting in the duplication of windows shown on the right. Unsurprisingly, this makes downstream processing to accurately identify specific building elements and find their edges and calculate their dimensions very difficult.

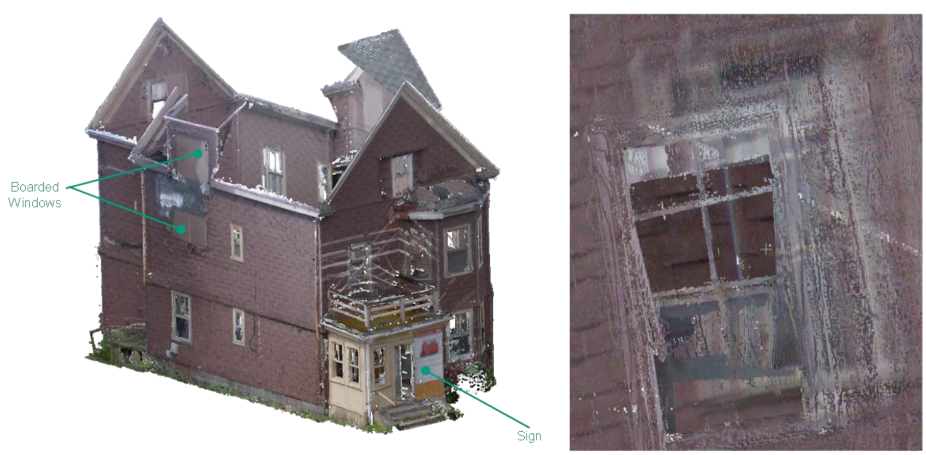

Figure 3. Example of a poorly scanned and registered building (left) resulting in indeterminate window location and geometry (right).

Once a unified point cloud exists, it still needs to undergo appreciable pre-processing before identification of building elements and extraction of their edges and dimensions can occur. As the left image of Figure 4 shows, the initial point cloud usually includes extensive data from objects surrounding that of interest. A limit box is used to isolate the area of interest (Figure 4, right), greatly reducing the quantity of remaining extraneous information.

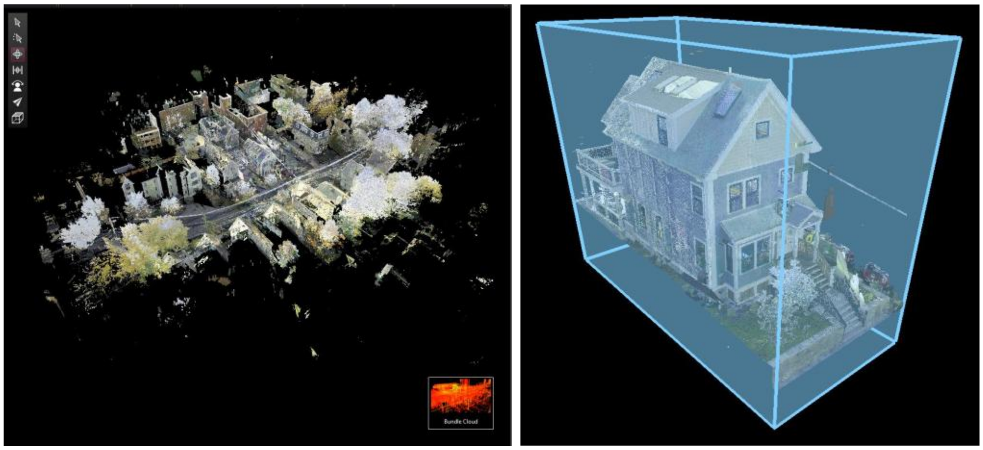

Figure 4. A registered point cloud for a single building before trimming (left) and with a limit box applied (right).

Figure 5 below shows an example of a registered point cloud ready for analysis for a single-family building. These are sizable files, on the order of 10 GB.

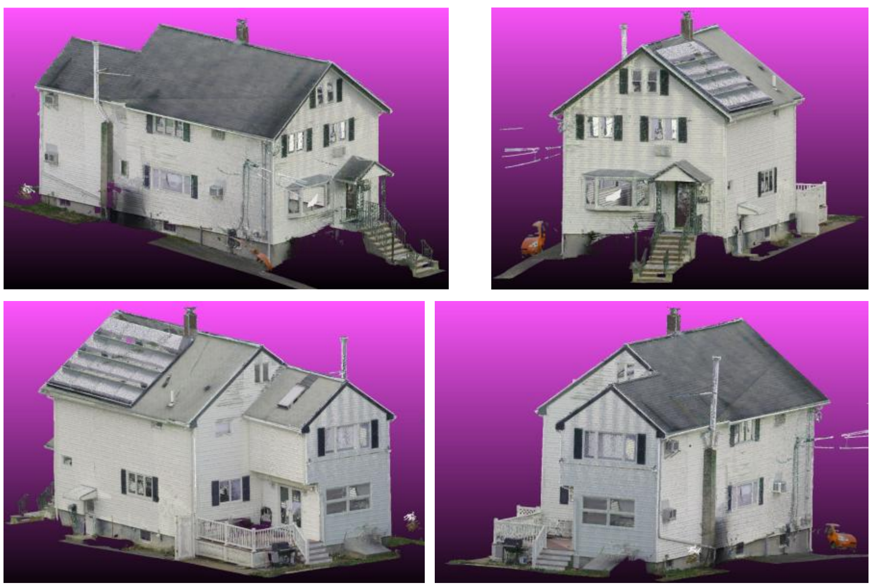

Figure 5. Example of a high-quality registered point cloud for a single-family building.

Further processing is required to address scanning artifacts, such as so-called "mixed-pixels." When scanning near the edge of a building feature, e.g., window frame, the scanner sometimes receives two return signals, e.g., one from the window frame and a second from the adjacent siding. Rather than generating a point on the window frame OR the siding, it creates a false point on the line between the two surfaces. As seen in Figure 6, the scan of a square edge protruding from the surface taken from the left side of the edge (Setup 3) accurately captures the shape on the side facing the scanner, but smears that on the far side where the scanner cannot "see" the interior corner. The same effect occurs when scanned from the right side (Setup 2), but this error is reduced with a head-on scan (Setup 1). The point cloud created from registering the point clouds from the three scans includes the mixed-pixel points (All), making it challenging to accurately extract the actual edges and calculate dimensions. We developed processes to identify and remove the false points, improving edge detection accuracy to ~1-2 mm.

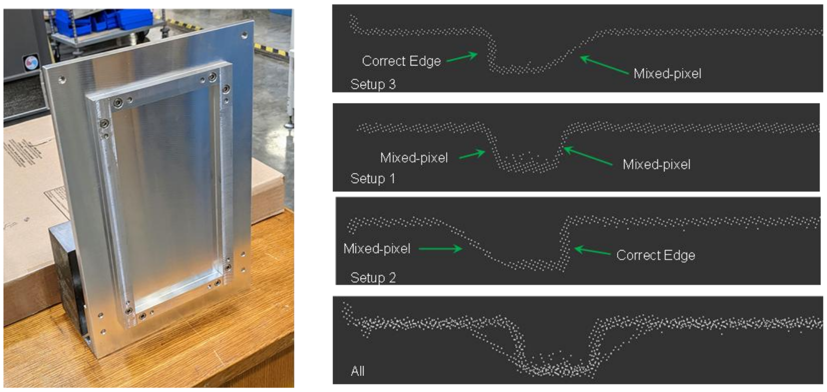

Figure 6. An example of how false mixed-pixel points are generated at edges from building scans.

Often, the scan does not capture some surfaces due to the shadow effect of the scanning process. For example, Figure 7 shows the case where the clapboard siding extends out beyond the foundation, preventing imaging of the underside by the scanner positioned higher than the foundation. Unsurprisingly, this can prevent precise location of the foundation-wall interface.

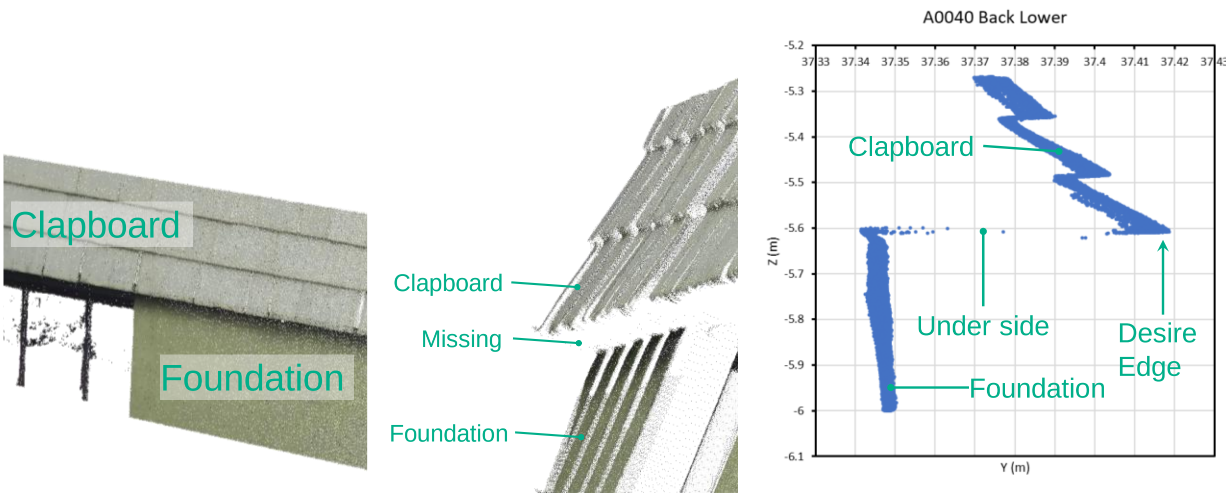

Figure 7. Example of a building scan not capturing a building surface "shadowed" due to the scanner location.

Another common challenge are objects that occlude the façade, ranging from those that can readily be moved (e.g., trash cans) to those that cannot (e.g., shrubbery). In the building residing use case, foliage that is too close to a building will be removed to provide workers access (and limit damage to the cladding). Often, some extraneous objects inevitably remain, and scene completion techniques are used to fill in the occluded region by inferring what would most likely exist in that specific context. Alternately, a S2B editor can manually complete the scenes.

Point Cloud Segmentation

After pre-processing the unified point cloud, point cloud segmentation (PCS) processes the point cloud and segments (i.e., groups) its points into different instances of relevant object classes. Examples of façade object classes include walls, windows, soffits, foundation, doors, etc. Typically, a neural network (NN) largely automates the PCS process. Large datasets exist to support NN training for segmenting two-dimensional images, where people have tagged (i.e., labeled) the individual points in images that serve as NN inputs. In contrast, there are many fewer segmented point-cloud data sets available (Selvakumar et al. 2025); this reflects the much greater time required to manually and accurately segment point clouds. We created our own training data set, with object classes defined for facades. In general, the accuracy of the segmentation process increases with the quality and consistency of all prior steps, training data set size, and the number of instances of different features in the training data set.

The lower two images in Figure 8 shows an example of a manually segmented point cloud not used for NN training, while the upper images show the results of the NN applied to that same point cloud. As expected, the NN produced less precise boundaries between features than manual segmentation, but tagged all object classes with approximately the correct size, shape, and location. Although the NN tagged some false segments, e.g., solar panels as "Roof" and some of the roof as "Soffit," the S2B algorithms reliably extract the soffit location (labeling solar panels as "roof" is not a concern for the façade application). This robustness reflects that our S2B algorithms only require approximate object locations to accurately find edges. The NN also identified an existing door in the foundation (View 2) that manual tagging missed.

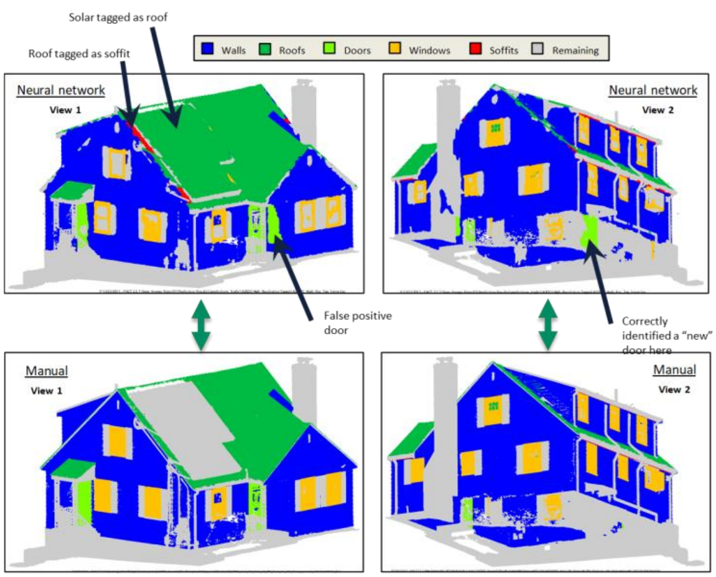

Figure 8. NN segmentation results for several object classes (above) as compared to manual segmentation (lower). The manually segmented point clouds from this building were not used for NN training.

Not infrequently, the NN finds a portion of other building objects or identifies different portions as multiple, separate objects (see Figure 9, left). To address this, we created tools to re-process the NN output to more accurately segment objects (Figure 9, right). This tool also supports manually deleting incorrect segments and adding new ones when something is missed.

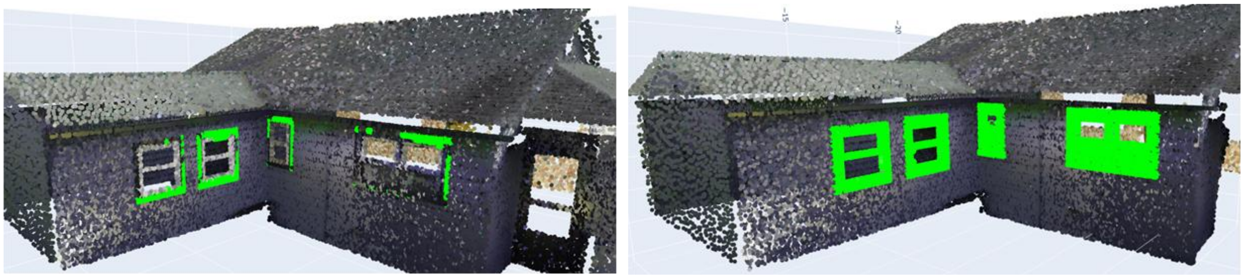

Figure 9. Examples of initial (left) and final after post-processing (right) NN segmentation results for windows.

We also tested the segmentation software in a home that was scanned and registered into a unified point cloud by another organization (see Figure 3 above) that posed several challenges:

- Lower point cloud densities;
- Lower scan densities on upper stories (same challenges);
- Poor scan registration, causing ~double-vision like duplication of features; and
- Boarded-up windows and significant trim damage, making it more challenging for the NN to identify and accurately segment instances of building features.

Despite problems with the scans, the NN identified almost all building features (Figure 10, left), which enabled S2B to find all but one of the edges (Figure 10, right).

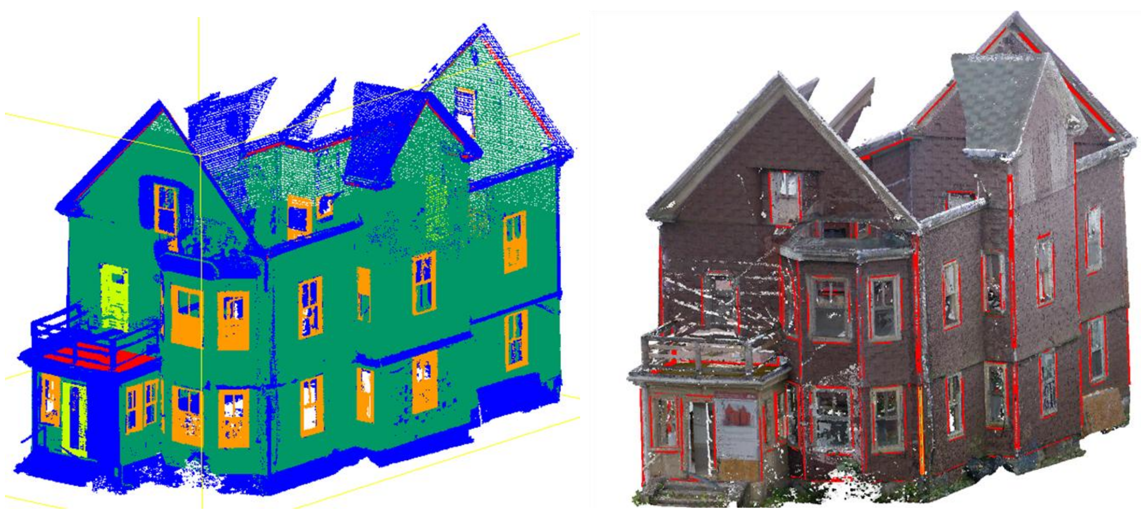

Figure 10. Neural network segmentation (left) and edge identification (right) results for a poorly scanned building.

Edge Detection, Fitting, Identification, and Panelization

Once the NN has identified all façade elements, the software performs geometric refinement. That is, it wants to recognize objects such as walls, windows, and doors AND localize their boundaries with high accuracy. We do this by using an edge detection and classification pipeline that operates on the segmented point cloud.

While segmentation provides approximate object regions, it is not sufficiently precise for prefabrication. Accurate edge localization is a critical step that presents several practical challenges. As discussed previously, scan noise and registration error affect the reliability of the underlying point cloud. In poorly scanned areas, measurement variability can obscure sharp transitions, and small registration offsets can produce “ghosted” geometry that appears as duplicate or shifted edges. Figure 11 below shows a close-up of a poorly scanned building.

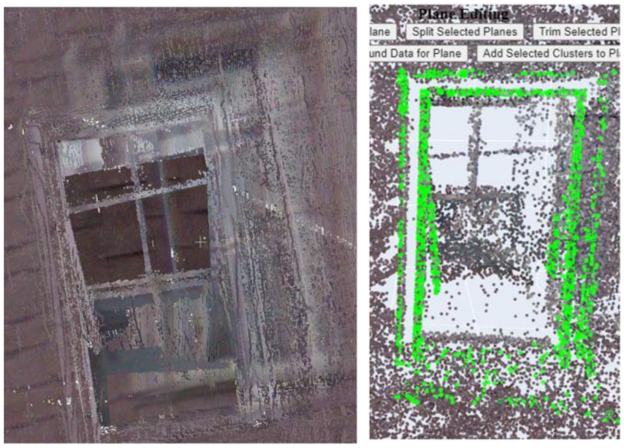

Figure 11. A poorly scanned and registered building results in duplication of a window (left), making identification of the actual window location very difficult (right).

Beyond data quality, the number of edges that need to be found can present challenges. Even the most basic buildings contain a surprisingly large number of edges, typically between 100 and 300 (see Figure 12) in the 60 structures we have analyzed, including many short or subtle features that must be detected consistently. Lastly, building edges are not uniform, with architectural styles, construction practices, renovations, and material aging and degradation introducing variation, irregularity, and small geometric abnormalities. Edge detection must perform reliably and deliver consistent dimensional accuracy in spite of these factors.

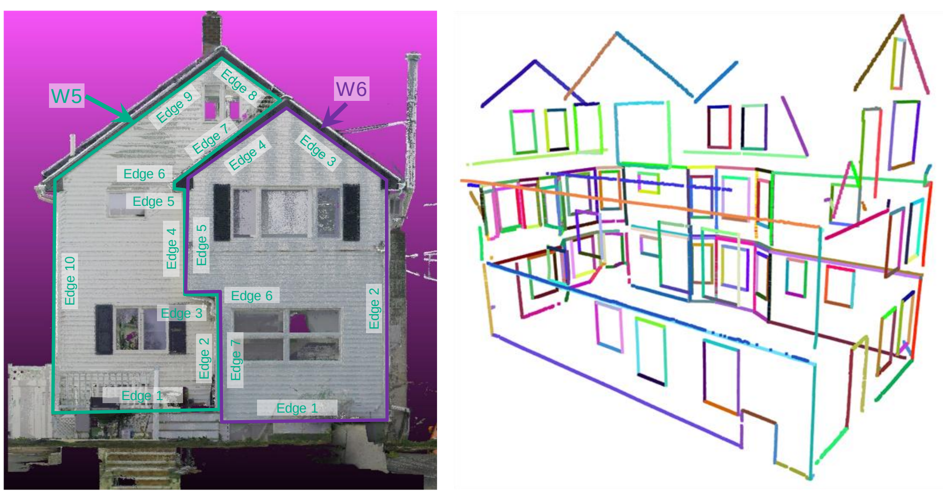

Figure 12 Manually labeled edges for one building (left) and edges found for another, more complex home (right).

The first stage of the edge detection pipeline treats point-cloud segmentation as a coarse localization step. The segmented point cloud identifies candidate regions for each object, providing an approximate spatial context for walls, windows, doors, and other façade elements. The software then “zooms in” on each localized region and performs a higher-resolution geometric analysis. The system re-examines the localized raw point data to resolve the true physical limits of each object. This refinement step isolates the structural transitions that define real edges and filters out ambiguities introduced by noise, partial occlusions, or imperfect labeling. The result is a set of geometrically precise edge locations that form the foundation for accurate dimensional extraction and reliable panel block generation.

After identifying the edge locations, the software fits them together to create coherent object boundaries. Individual edge segments are reconciled with neighboring edges so that each window, door, and wall has a consistent, closed boundary. We extended this process across the entire building, ensuring that connected walls intersect cleanly and that corners align properly. The result is a unified wireframe representation of the structure constructed from geometrically refined edges that enables accurate extraction of object positions and dimensions.

The edge processing techniques used can have a significant impact on the dimensional accuracy extracted in the final step. Figure 13 shows the results for two edge finding algorithms we tested for a window edge, the most common edge type encountered in most buildings, where the blue points represent points from a narrow slice through the point cloud. Our original edge-finding approach converged on the red points, representing the actual window edge surface within ~±4-6 mm, while the enhanced algorithms found the green points within ~±1 mm of the actual edge.

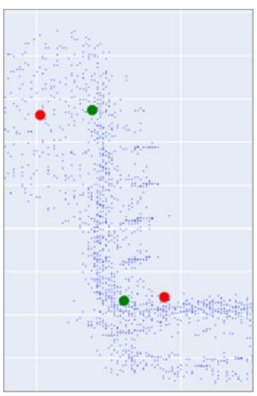

Figure 13. Example of how edge fitting technique impacts S2B dimension accuracy for windows. The window edge projects on the y-axis; units for x and y intervals are both 6.4 mm, but are shown on different scales

We then classified edges based on their associated segmented object and geometric role (e.g., bottom of window, soffit). This structured labeling is essential for downstream processing, as different edge types are treated differently during fabrication planning, i.e., panelization.

Although the edge detection pipeline is automated, we developed a lightweight edge-editing tool to address rare failure cases. In situations involving poor scans or significant registration issues, an edge may be missing or duplicated. The editing interface allows a user to quickly adjust or insert edges directly within the wireframe, avoiding the need for time-intensive manual remodeling of the entire building model.

The final wireframe feeds into the panelization module, which generates manufacturable panel blocks for retrofit installation. This stage applies manufacturing constraints, such as allowable panel dimensions, while also considering overall façade composition. Because panel boundaries are derived directly from the detected edges, dimensional accuracy at the edge-detection stage directly affects fabrication fit and installation quality.

Application of S2B to Five Structures

We applied the S2B process to five structures and compared the S2B dimensions to those measured using a tape measure, laser tape measure, and a surveyor's total station (TS). The acceptable dimensional accuracy of a S2B process depends on the needs of its target application. For prefabricated exterior wall recladding, the S2B error needs to be less than what the cladding system design can accommodate (based on a tolerance stack analysis) and still function effectively (Canmet Energy 2023).

It is important to note that none of the measurements are true "ground-truth" dimensions, each has its own sources of potential error. That is S2B has scan registration and edge detection errors, tape measures have sag and thermal expansion, and TSs have station-to-station alignment and edge detection. We wanted to build confidence in the S2B process, ideally the measurement techniques would yield very similar values with a difference less than the target accuracy of ±6.4 mm (¼ inch) for the insulated panel block recladding system we developed (Briggs et al. 2022).

Results. The S2B matched tape measurements within tolerance for all 48 dimensions measured using both techniques, with an average absolute difference of 2.5 mm, while the S2B matched total station measurements within tolerance for 43 of 48 dimensions (absolute average difference of 3.3 mm[1]). Of the five out of tolerance, three exceeded it by <1mm and the other two are TS measurement errors. With a few exceptions where the TS measurements were clearly in error, the tape (manual and laser) and TS measurements always agreed within a few millimeters, i.e., an average absolute difference for 44 dimensions of 1.7mm (~1/16").[2] Discussions of the results for each structure follows (each has a unique identification code, e.g., A0001, A0019, etc.).
A0001: The S2B and tape measure values all agree within ±5.5 mm for the shed.
A0003: The S2B and tape measurements all agree within <5mm, while there's a 7mm difference between both and the TS measurements for one height measurement (D2). However, the TS measurement appears to be the outlier, i.e., the tape measure and S2B are closer to each other, we conclude that S2B met the ±6.4 mm accuracy target for this building.

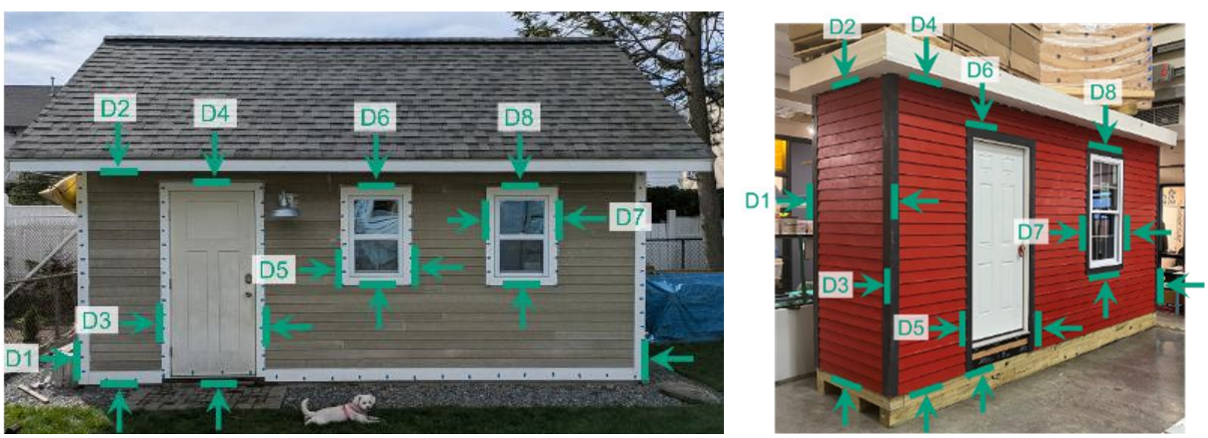

Figure 14. Images and building dimensions evaluated for A001 (left) and A003 (right).

[1] Excludes two measurements with known TS error.
[2] Excludes two measurements with known TS error and two w/o TS measurement

Table 1. Comparison of A0001 scan-to-BIM (S2B), total station (TS), and tape measurements.

			S2B (m)	TS (m)	Tape (m)	S2B-TS (mm)	S2B-Tape (mm)
Wall 1	Width	D1	6.181	6.186	6.186	-4.8	-5.5
	Height	D2	2.475	2.471	2.472	3.7	3.3
Door 1	Width	D3	1.109	1.113	1.114	-4.1	-5.4
	Height	D4	2.192	2.188	2.191	3.7	1.3
Window 1	Width	D5	0.781	0.782	0.783	-0.8	-1.3
	Height	D6	1.087	1.083	1.082	3.4	4.4
Window 2	Width	D7	0.782	0.783	0.783	-0.7	-0.6
	Height	D8	1.088	1.084	1.083	3.7	4.8

Table 2. Comparison of A0003 S2B, total station (TS), and tape measurements.

			S2B (m)	TS (m)	Tape (m)	S2B-TS (mm)	S2B-Tape (mm)
Wall 1	Width	D1	1.246	1.246	1.245	0.5	1.5
	Height	D2	2.645	2.652	2.645	-7.0	0.0
Wall 2	Width	D3	5.334	5.334	5.337	-0.1	-2.5
	Height	D4	2.645	2.650	2.645	-4.8	0.5
Door	Width	D5	1.094	1.089	1.090	4.6	4.0
	Height	D6	2.351	2.357	2.354	-5.8	-3.0
Window	Width	D7	1.042	1.040	1.040	2.0	2.0
	Height	D8	1.625	1.623	1.623	1.6	2.5

A0018: We found the lowest agreement between the S2B and other measurement techniques for this building, with 9 of 11 measurements within ±6.4 mm (see Table 3). Two measurements exceeded the target by <1 mm; given the sources of error in all the measurements, it is not clear that those differences are truly significant.

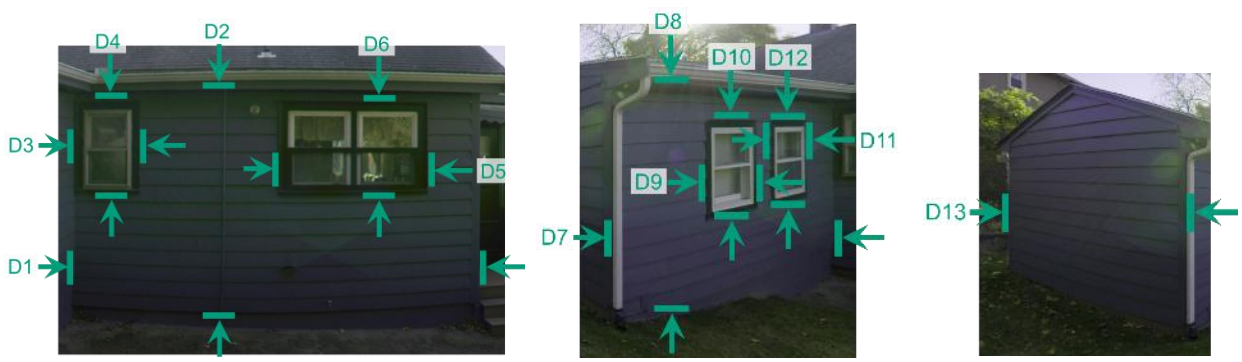

Figure 15. Images and building dimensions evaluated for A0018.

Table 3. Comparison of A0018 S2B, total station (TS), and tape measurements.

			S2B (m)	TS (m)	Tape (m)	S2B-TS (mm)	S2B-Tape (mm)
Wall 1	Width	D1	4.941	4.946	4.947	-4.6	-6.0
	Height	D2	2.688	2.681	2.682	7.2	6.0
Wall 2	Width	D7	4.913	4.908	4.910	5.2	3.5
	Height	D8	2.315	2.309	2.314	6.3	1.5
Wall 3	Width	D13	4.32	4.319	4.321	1.0	-1.0
Window 1	Width	D3	0.81	0.808	0.809	2.0	1.5
	Height	D4	1.11	N/A	1.114	N/A	-3.5
Window 2	Width	D5	1.805	1.801	1.803	3.9	2.0
	Height	D6	1.106	N/A	1.110	N/A	-4.0
Window 3	Width	D9	1.034	1.027	1.032	6.7	2.5
	Height	D10	1.106	1.111	1.111	-4.8	-5.0
Window 4	Width	D11	1.04	1.037	1.040	2.8	0.0
	Height	D12	1.111	1.115	1.114	-3.5	-3.0

A0019: The 10 TS and S2B measurements all agreed within the target tolerance (see below for walls 1, 2, and 4). However, two of the wall 4 TS measurements, D8 and D9, are off by almost 25 mm. Since the tape and S2B values match closely, the TS measurement is likely in error. One other point to note are the corrections applied to this building and other with shingle or clapboard siding that lack a corner post. The specified offsets can be readily calculated in the S2B software, e.g., using check-boxes indicating the siding and corner type.

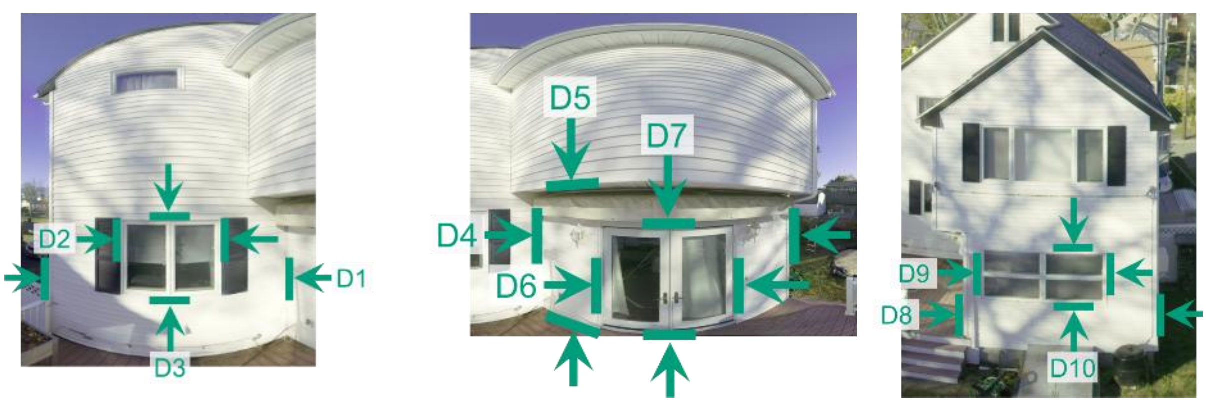

Figure 16. Images and building dimensions evaluated for A0019. Note that the apparent curvature in the images is an artifact of the wide field of view used to show the full façade.

Table 4. Comparison of A0019 S2B, total station (TS), and tape measurements.

			S2B (m)	TS (m)	Tape (m)	S2B-TS (mm)	S2B-Tape (mm)
Wall 1	Width lower	D1*	3.510	3.509	3.510	1.7	0.3
Window 1	Width	D2	1.218	1.216	1.214	2.0	4.0
	Height	D3	1.036	1.041	1.040	-5.4	-4.0

			S2B (m)	TS (m)	Tape (m)	S2B-TS (mm)	S2B-Tape (mm)
Wall 2	Width	D4*	4.311	4.310	4.310	1.7	1.3
	Height	D5**	2.651	2.651	2.653	0.0	-1.5
Door 1	Width	D6	1.769	1.767	1.769	1.5	0.0
	Height	D7**	2.157	2.161	2.158	-3.8	-1.0
Wall 4	Width lower	D8	3.778	3.801	3.781	-23.5	-3.0
Window 2	Width	D9	2.440	2.415	2.439	24.5[#]	1.0
	Height	D10	1.231	1.232	1.232	-1.0	-1.0

* The TS measurement was based on the clapboard peaks, while the S2B measurement finds the middle of the sawtooth. We applied an offset of 6.7mm to correct for this systematic difference.

**The TS measurement is based on the decking board surface, but the S2B measurement is based on an edge above the decking boards. We applied a 25mm offset to correct for this systematic difference.

[#] Given the large difference between the TS and both the tape and S2B measurements, we conclude the TS measurement is in error.

A0020: The S2B and TS values agreed within ±5.3 mm once specifying the corner design.

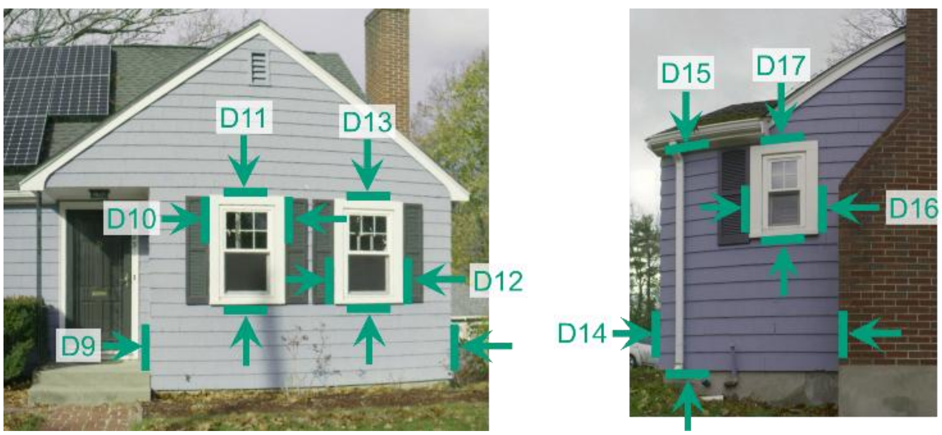

Figure 17. Images and building dimensions evaluated for A0020.

Table 5. Comparison of A0020 S2B, total station (TS), and tape measurements.

			S2B (m)	TS (m)	Tape (m)	S2B-TS (mm)	S2B-Tape (mm)
Wall 3	Width	D9*	4.192	4.191	4.194	0.4	-2.5
Window 2	Width	D10	0.984	0.988	0.985	-4.4	-1.3
	Height	D11	1.403	1.405	1.406	-2.0	-2.7
Window 3	Width	D12	0.985	0.991	0.987	-5.3	-1.5
	Height	D13	1.401	1.403	1.403	-1.9	-2.2
Wall 4	Width	D14*	2.019	2.018	2.018	1.0	1.1
	Height	D15	2.604	2.601	2.600	3.5	4.5
Window 4	Width	D16	0.704	0.709	0.707	-4.7	-2.9
	Height	D17	1.117	1.112	1.113	5.3	4.0

* A0020 lacks corner posts, i.e., the wood shingles fully extend to each corner. The TS measurement is based on the shingle peaks, while the S2B measurement finds the middle of the sawtooth. Thus, we applied a 5mm offset per side to correct for this systematic difference.

Since performing the testing on these five structures, we have continued to improve the S2B algorithms, particularly for edge fitting and dimensioning, to further improve accuracy. In addition, we developed a graphical user interface (GUI) that enables the user to inspect and edit the results during the S2B process. Together, this has led to an increase in accuracy from ~±6mm to ~±4 mm for walls and windows/door dimensions, respectively. Note that these accuracy values reflect the tolerances of values, i.e., that *all* measurements are within plus-minus those values, instead of, e.g., standard deviations (where ~32% of measurements would fall outside plus-minus those values). Concurrently, the computational time on a high-performance personal workstation has decreased around five-fold to around 15 minutes.

Conclusions and Recommendations

Effective scan-to-BIM processes have the potential to help realize the vision of recladding walls with prefabricated highly insulated panels. We applied the S2B process to five buildings where we compared the S2B dimensions to those measured using a tape measure, laser tape measure, and a surveyor's total station (TS). Overall, the S2B matched tape measurements within ±6.4 mm (¼ inch) for all 48 dimensions measured using both techniques, while the S2B matched total station measurements within tolerance for 43 of 48 dimensions. Of the five out of tolerance, three exceeded the tolerance by <1mm and the other two were TS measurement errors. This compares favorably with the dimensional accuracy found by other researchers. For example, Maldonado et al. (2023) developed an S2B process and applied it to a duplex home with simpler façade. They compared the S2B and manual laser measurements for 18 windows and found a mean absolute difference of ~4 mm, with differences for four measurements exceeding 10 mm (they did not compare façade measurements). Another team used S2B to measure interior wall and ceiling dimensions and obtained differences from 1 to 16 mm, with an average of around 9 mm (Esfahani et al. 2021). Finally, a comparison of measurements for a test facade found S2B was "accurate to within 1 cm" (10 mm; Egan, Fouquet, and Harris 2023).

We conclude that the promise of scan-to-BIM for this use case can be realized, i.e., can yield very precise building façade measurements, when all steps of the scan-to-BIM process are implemented effectively. This requires achieving high quality at every step of the process:

1. Scanning: A sufficient number of high-quality scans are obtained from enough locations to adequately capture all surfaces of all facades;
2. Scan Registration and Pre-processing: To create a unified point cloud that precisely registers points from different scans while minimizing the impact of outlier points, mixed-pixel points, scan shadows, and scan occlusions, etc., all of which compromise the effectiveness of subsequent downstream steps.
3. Point Cloud Segmentation: Accurately groups points with the correct object class, e.g., walls, windows, doors, soffit, foundation, etc. and does not miss instances of each. Performance should be robust across the range of architectural styles, features, etc.
4. Edge Detection, Fitting, Identification, and Panelization: Algorithms that analyze the segmented point clouds precisely identify and locate all the edges of all façade elements, in a way that is similarly robust across the highly heterogeneous building sector.

Acknowledgements

The work presented in this paper is funded in part by the U.S. Department of Energy Building Technologies Office Advanced Building Construction (ABC) Program under Contract # DE-EE0009066. We extend our gratitude to Sven Mumme and Jonathan Cohen of DOE-BTO and Eric Werling, former DOE-BTO Building America Program Director, for their support and many fruitful discussions. We also thank the Massachusetts Clean Energy Center (MassCEC) AmplifyMass program for their funding support. Finally, we thank Evan Smith of Highland Park Technology for sharing examples of problematic building scans *not* conducted by his company.

References

Borkowski, A.S. and A. Kubrat. 2024. “Integration of Laser Scanning, Digital Photogrammetry and BIM Technology: A Review and Case Studies.” *Eng*. Vol 5, pp. 2395–2409.

Briggs, J., A. Sharpe, H.C. Fennell, K. Roth, and A. Sharon. 2022. “Digitalization of Deep Wall Retrofits: An Integrated Insulated Panel Block (PB) System and Process.” *Proc. ACEEE Summer Study on Energy Efficiency in Buildings*. August.

Building Science Corporation. 2013. “Mass Save Deep Energy Retrofit Builder Guide.”

Esfahani, M.E., C. Rausch, M.M. Sharif, Q. Chen, C. Haas, and B.T. Adey. 2021. “Quantitative investigation on the accuracy and precision of Scan-to-BIM under different modelling scenarios.” *Automation in Construction*. vol. 126. March.

Gilmour, L. and E. Stroulia. 2022. “Ortho-photogrammetry for prefabricated energy-efficiency retrofits.” *Automation in Construction*, vol. 134.

Highland Park Technologies. 2026. https://www.hiparktech.com/ .

Maldonado, B.P., N.W. Hayes, and D.E. Hun. 2023. “Automatic point Cloud Building Envelope Segmentation (Auto-CuBES) using Machine Learning.” *Proc. 40th International Symposium on Automation and Robotics in Construction*. pp. 48-55. July.

PNNL. 2022. “Wall Upgrades for Energy Retrofits: A Techno-Economic Study.” Final Report by Pacific Northwest National Laboratory. PNNL-32231.

Rauch, L. and T. Braml. 2023. “Semantic Point Cloud Segmentation with Deep-Learning-Based Approaches for the Construction Industry: A Survey.” *Appl. Sci.* vol. 13.

Signetron. 2026. https://signetron.com/pater/ .

Selvakumar, B. Y. Liu, N.W. Hayes, D.E. Hun, and B.P. Maldonado Puente. 2025. “Deep Point Cloud Building Envelope Segmentation (DeeP-CuBES) using Deep Learning.” *Proc. 42nd International Symposium on Automation and Robotics in Construction*. pp. 1425-1432. July.

Xiong, X., A. Adan, B. Akinci, and D. Huber. 2013. “Automatic creation of semantically rich 3D building models from laser scanner data.” *Automation Construction*, vol. 131. pp. 325–337.